Investigation of the potential of using TiO_2 nanoparticles as a contrast agent in computed tomography and magnetic resonance imaging

Hiroaki Akasaka[a] *, Naritoshi Mukumoto[a], Masao Nakayama[b], Tianyuan Wang[c], Ryuichi Yada[c], Yasuyuki Shimizu[c], Sachiko Inubushi[c], Katsusuke Kyotani[d], Keisuke Okumura[d], Masanori Miyamoto[d], Ai Nakaoka[c], Kenta Morita[e], Yuya Nishimura[e], Chiaki Ogino[e] and Ryohei Sasaki[a]

[a]Division of Radiation Oncology, Kobe University Hospital, Chuo-ku Kobe, Hyogo 650-0017, Japan

[b]Division of Medical Radiations School Health & Biomedical Sciences, RMIT University, Plenty Road, Bundoora, Victoria 3083, Australia

[c]Division of Radiation Oncology, Kobe University Graduate School of Medicine, Chuo-ku Kobe, Hyogo 650-0017, Japan

[d]Center for Radiology and Radiation Oncology, Kobe University Hospital, Chuo-ku Kobe, Hyogo 650-0017, Japan

[e]Department of Chemical Science and Engineering, Graduate School of Engineering, Kobe University, 1-1 Rokkoudaicho, Nadaku, Kobe, Hyogo 657-8501, Japan

*Correspondence to: Hiroaki Akasaka, Division of Radiation Oncology, Kobe University Hospital, Chuo-ku Kobe, Hyogo 650-0017, Japan.

Tel: +81-78-382-5687; Fax: +81-78-382-6734.

E-mail: akasaka@harbor.kobe-u.ac.jp (H. Akasaka)

Keywords: Nanoparticle, Radiotherapy, Radiation diagnosis, Theranostic drug, titanium dioxide nanoparticles

24 **ABSTRACT**

25 Nanoparticles (NPs) are useful for radiotherapy. Currently, efforts are underway globally for the development of
26 novel titanium dioxide NPs (TiO_2-NPs) that exhibit both contrast effects and anti-tumor effects. In this study, the
27 image contrast properties of TiO_2-NPs were evaluated using a clinical magnetic resonance imaging (MRI)
28 system and a clinical computed tomography (CT) scanner, as the use of TiO_2-NPs as an anti-cancer agent has
29 been reported in several reports. An obvious difference in visualization was observed between the control and
30 TiO_2-NP samples on T_2-weighted images. These results suggest that TiO_2 can potentially be used as a novel
31 theranostic drug with radiosensitizing ability and radiological diagnostic ability, through modification of
32 chemical groups on its surface, and as a component of drug delivery systems.

33 Keywords: Nanoparticle, Titanium oxide, Theranostic, MRI, CT, Radiotherapy

34 **Background**

35 Radiation therapy is one of the major treatment modalities for cancer, in which ionizing radiation is
36 used to kill cancer cells (Akasaka et al. 2016). An increased radiation dose would result in more effective
37 elimination of the cancerous tissue. However, in some cases, the radiation dose cannot be increased due to the
38 possibility of damage to nearby functional and healthy tissues, and this limits the efficacy of the treatment
39 (Bump et al. 2003; Akasaka et al. 2014; T. Ruba et al. 2018); consequently, currently only a few effective
40 radiotherapy techniques are available, and novel strategies need to be explored (Akasaka et al. 2014). Recently,
41 there has been a rapid increase in the use of nanoparticles (NPs) for biological applications, and there is potential
42 for their use in the diagnosis and treatment of human cancer (Yezhelyev et al. 2006; Kim et al. 2010; Service
43 2005).

44 NPs have been extensively studied for their potential applications in the scientific field due to their
45 unique electrical, magnetic, and visibility and their versatile functionality. Biomedical applications of NPs have
46 attracted considerable attention because NPs are expected to improve medical diagnosis and treatment. Moreover,
47 various NPs have been used as contrast agents in magnetic resonance imaging (MRI) and computed tomography
48 (CT). Currently, the NPs under development for clinical imaging include gold NPs for X-ray contrast (Hainfeld
49 et al. 2006), magnetic NPs for MRI enhancement (Fang and M. Zhang 2009), and also hybrid NPs containing
50 iron oxide and gold in polymer coating, which can serve as contrast agents for both CT and MRI (Kim et al.
51 2011).

In addition to their potential applications in imaging, NPs are also being investigated for their potential application in cancer therapy (Chatterjee et al. 2008; Wilson and Patterson 2008; Garnica-Garza 2009). They offer similar advantages over other contrast agents in this area as in imaging. In addition, it is also possible to design NPs that can selectively accumulate in cancer cells, thereby providing targeted treatment that may not be possible with conventional techniques (Chatterjee et al. 2008).

Several NPs made from titanium dioxide (TiO_2-NPs) have been investigated worldwide for their potential application in cancer therapy. Some studies have shown that irradiation of TiO_2-NPs generates free-radicals that facilitate the spontaneous generation of reactive oxygen species (ROS) (Jin et al. 2011; Townley et al. 2012; Yin et al. 2012; Babaei and Ganjalikhani 2014). In vivo studies using TiO_2-NPs have demonstrated a significant decrease in tumor volume when these NPs are irradiated with 200-kV X-rays (Nakayama at al. 2016). Moreover, recent in vitro studies on glioma cells have demonstrated the potential use of such NPs for photodynamic therapy (Yamaguchi et al. 2010). Ultrasonic stimulation of TiO_2-NPs has been shown to kill NP-impregnated glioma cells in a manner similar to that of ultraviolet stimulation of TiO_2-NPs (Allison et al. 2010). Other studies have shown that TiO_2-NPs are also essentially non-toxic (Bischoff and Bryson 1982; Bernard et al. 1990; Fabian et al. 2008) and hence hold considerable promise as cancer therapy agents.

Currently, the development of novel TiO_2-NPs with both the potential to be used as a contrast agent and as well as to produce anti-tumor effects is under investigation all over the world. Although several studies have investigated the imaging properties of TiO_2-NPs, they have all used TiO_2-NPs that have been chemically modified. To our knowledge, the imaging properties of unmodified TiO_2-NPs have not been investigated thus far. Hence, in this study, we investigated the visibility of TiO_2-NPs using clinical MRI and CT scanning in an attempt to determine their image contrast properties.

2. Materials and methods

2.1. Transmission electron micrography and dynamic light scattering of nanoparticle "TiO_2"

The TiO_2-NPs used in this study were purchased from Ishihara Sangyo, Ltd. (Osaka, Japan). The size and morphology of the TiO_2-NPs were evaluated using a transmission electron microscope (TEM) (JEM-1200EX, JEOL Ltd., Tokyo, Japan) as described previously (Srivastava et al. 2013). The TEM images were obtained at an acceleration voltage of 80 kV. Dynamic light scattering (DLS) was performed using a Malvern

Zetasizer ZS (Malvern Panalytical Ltd, Malvern, United Kingdom) to estimate the hydrodynamic diameter of the TiO_2-NPs.

2.2. Magnetization measurement

The variation in the magnetic moment was carried out by altering the applied field from 10,000 Oe to 10,000 Oe at 25.2°C. This measurement was performed by Toei Industry Co., Ltd. (Tokyo, Japan). To correct for the diamagnetic contribution of the sample tube, the magnetic moment of the empty sample tube and sample holder was subtracted from the data sets; however, due to the high magnetization values obtained from the NP sample, the contribution of the sample tube and holder was considered negligible and was ignored.

2.3. Cell culture and viability assessment

MIAPaCa-2 cells were obtained from the American Type Culture Collection (Manassas, VA, USA) and cultured in Roswell Park Memorial Institute 1640 medium supplemented with 10% fetal bovine serum, penicillin (100 U/mL), and streptomycin (100 μg/mL). The anti-tumor effect, in combination with the radiation treatment, was assessed with the colony forming assay. For the colony forming assay, MIAPaCa-2 cells were treated with 0.1 mg/mL TiO_2-NPs or saline for 1 h, and then exposed to 0, 2, 4 and 8 Gy of radiation. After 9–12 days, colonies were fixed with a solution of 10% methanol and 20% acetic acid, stained with methylene blue, and counted under a light microscope.

2.4. X-ray irradiation

X-ray irradiation was performed using an MBR-1505R2 instrument (Hitachi, Tokyo, Japan) at a voltage of 150 kV and a current of 5 mA with a 1-mm-thick aluminum filter (0.5 Gy/min at the target) for in vitro studies.

2.5. CT imaging

CT images were acquired using Aquilion LB (TOSHIBA Medical Systems, Tochigi, Japan). Imaging parameters were as follows: slice thickness, 1.0 mm; tube energy, 120 kVp, 300 mA; field of view (FOV), 320 mm; matrix, 512 × 512. CT data were analyzed using the Hounsfield units (HU) for regions of interest. The concentrations of the TiO_2-NPs used are shown in Table 1.

2.6. MR imaging

MR imaging experiments were performed on a 3.0 T MR unit (Ingenia, PHILIPS, Amsterdam, Netherlands). Two pulse sequences were used. One was a T_1-weighted SE-XL/90 sequence with the following parameters: relaxation time (TR) = 4000 ms; echo time (TE) = 16 ms; FOV = 260 mm; matrix = 512 × 512; and slice thickness = 3 mm. the other was a T_2-weighted FSE-XL/90 sequence with the following parameters: TR = 4000 ms; TE = 100 ms; FOV = 260 cm; matrix = 512 × 512; slice thickness = 3 mm. The concentrations of the TiO_2-NPs used are shown in Table 1.

2.7. Statistical analysis

Data are presented as mean ± standard error. Differences between groups were evaluated with the Student's t test. Data were considered statistically significant at $P < 0.05$.

3. Results

3.1. TEM and DLS

Considering enhanced permeability and retention effects of TiO_2-NPs, we aimed to prepare NPs with a size of less than 100 nm (Maeda et al. 2000; Perrault et al. 2009; Huo et al. 2013). The diameter of the TiO_2-NPs was determined to be approximately 50 nm using TEM (Fig. 1a). Consistent with the TEM images, the diameter of the TiO_2-NPs was determined to be approximately 50-100 nm using DLS, with a narrow unimodal size distribution (Fig. 1b).

3.2. Magnetic properties

Fig. 2 shows the magnetization of TiO_2-NPs at 25.2°C. The saturation magnetization (Ms) value for TiO_2-NPs was 9.711×10^{-4} emu and the remanence (Mr) was 4.269×10^{-6} emu. The TiO_2-NPs showed weak diamagnetic behavior.

3.3. Cell viability assessment

The colony forming assay results revealed fewer MIAPaCa-2 cell colonies on treatment with the combination as compared to irradiation alone (*$P < 0.05$ and **$P < 0.1$) (Fig. 3).

3.4. CT imaging and MR imaging

The CT numbers for the control group and for the different concentrations of TiO_2-NPs used are shown in Fig. 4(a) and Table 1. Contrast-enhanced CT images are shown in Fig. 4(b). The uncertainty in each

measurement (represented by the standard deviation of the Hounsfield unit measurement) was 0.3 HU. The sensitivity of the TiO_2-NPs to detection with MRI was determined. The T_1 and T_2 values for the control group and for the different concentrations of TiO_2-NPs used are shown in Fig. 4(c, e) and Table 1. Contrast-enhanced T1W and T2W images are shown in Fig. 4(d, f) and Table 1.

4. Discussion

NPs are being studied all over the world, and have the potential to be used as novel therapeutic agents for cancer. In particular, TiO_2-NPs have great potential for this application. For example, they can be used as anti-tumor agents by incorporating them in drug delivery systems. Therefore, in this study, we investigated the visibility of TiO_2-NPs using clinical MRI and CT scanning in an attempt to determine their image contrast properties.

No obvious aggregation was observed in the representative TEM image of the NPs depicted in Fig. 1a. Fig. 1b shows the size distribution of the NPs. The diameter was about 50–100 nm, which is suitable for the enhanced permeability and retention effects.

Leon Smith et al. indicated the CT value of their TiO_2-NPs in their publication and concluded that a TiO_2-NP concentration of greater than 15 mg/mL produced detectable changes in the CT number (Leon et al., 2012). In our study, the maximum concentration used was 5.0 mg/mL. Because of the low concentration of TiO_2-NPs, there was no difference in the imaging properties between the TiO_2-NPs and the control sample in our CT measurements; a gradual increase in CT value was observed in the investigated concentration range. In general, the atomic number of water is nearly 7, and that of the bone is nearly 20 because bone is composed almost entirely of calcium. In this study, the visualization in TiO_2-NPs and control samples was almost the same because of the low concentration of TiO_2-NPs. Hence, for TiO_2-NPs to be used for enhancement in MRI, their concentration in the tumor needs to be increased.

As shown in Fig. 2, TiO_2-NPs exhibited paramagnetic properties. This property is same as that of the small particulate gadolinium oxide (SPGO) enhancement agent (Gholamreza et al., 2012). Our results indicated that these findings regarding TiO_2-NPs are in line with the findings of previous research.

In magnetization measurements, TiO_2-NPs were observed to be weakly diamagnetic. On MRI, the imaging properties showed no difference between control and TiO_2-NPs on T_1-weighted imaging. However, the sensitivity to detection by MRI improved at higher concentrations of TiO_2-NPs, and there was a significant

difference in the T_2 value between control and TiO_2-NP samples at higher concentrations of TiO_2-NPs. These results show that TiO_2-NPs offer great potential for use in T_2-weighted MRI. As shown in Fig. 4(f), T_2-weighted images change drastically in signal intensity with an increasing TiO_2-NP concentration, indicating that TiO_2-NPs generated MRI contrasts on transverse (T_2) proton relaxation time-weighted sequences. Fig. 4(e) shows the relaxation rate $1/T_2$ as a function of TiO_2 concentration in TiO_2-NPs. The relaxation rates varied linearly with the titanium concentration, according to the following equation:

$$1/T_2 = 1/T_2^0 + r_2[TiO_2]$$

where $1/T_2$ is the observed relaxation rate in the presence of TiO_2-NPs, $1/T_2^0$ is the relaxation rate of pure water, $[TiO_2]$ is the concentration of TiO_2-NPs, and r_2 is the transverse relaxivity, which represents the efficiency of TiO_2-NPs, as a contrast agent shortens the proton relaxation times. The r_2 value of TiO_2-NPs was 5×10^{-4} $mg/mL^{-1}s^{-1}$. In addition, Fig. 4(c) shows the relaxation rate $1/T_1$ as a function of TiO_2 concentration in TiO_2-NPs. The relaxation rates were stable with the titanium concentration, according to the following equation:

$$1/T_1 = 1/T_1^0 + r_1[TiO_2]$$

where $1/T_1$ is the observed relaxation rate in the presence of TiO_2-NPs, $1/T_1^0$ is the relaxation rate of pure water, $[TiO_2]$ is the concentration of TiO_2-NPs, and r_1 is the longitudinal relaxivity, which represents the efficiency of TiO_2-NPs, as a contrast agent shortens the proton relaxation times. The r_1 value of TiO_2-NPs was 1×10^{-5} $mg/mL^{-1}s^{-1}$, suggesting that TiO_2-NPs are superior as a T_2-shortening agent than as a T_1-shortening agent. Additionally, TiO_2-NPs exhibit anti-tumor effect when combined with radiation, as shown in Fig.3. The result of the colony-forming assay indicated the radiosensitizing potential of TiO_2-NPs similar to that of the reported novel radiosensitizer, titanium peroxide NPs (TiOx-NPs) (Nakayama at al. 2016).

5. Conclusions

In summary, TiO_2-NPs offer considerable promise for use as contrast agents in MRI, especially T_2-weighted MRI. Our previous study showed that TiOx-NPs have anti-tumor effect (Nakayama at al. 2016). In this study, we observed that TiO_2-NPs that is used for preparing titanium peroxide also have anti-tumor effects. Additionally, the results show that titanium dioxide also exhibits imaging visibility. Thus, they have the potential to be used as novel theranostic drugs with radiosensitizing and radiological diagnostic abilities via modification of the chemical groups on their surface and use in conjunction with drug delivery systems. The findings of the present study indicate that using TiO_2-NPs can be an effective strategy for radiation treatment and cancer

188 diagnosis. Future clinical applications of those NPs require rigorous surface engineering and careful toxicity
189 evaluation.

190

References

Akasaka H, Mizushina Y, Yoshida K, Ejima Y, Mukumoto N, Wang T, Inubushi S, Nakayama M, Wakahara Y, Sasaki R (2016) MGDG extracted from spinach enhances the cytotoxicity of radiation in pancreatic cancer cells. Radiat Oncol 11(1):153

Akasaka H, Sasaki R, Miyawaki D, Mukumoto N, Sulaiman NS, Nagata M, Yamada S, Murakami M, Demizu Y, Fukumoto T (2014) Preclinical evaluation of bioabsorbable polyglycolic acid spacer for particle therapy. Int J Radiat Oncol Biol Phys 90(5):1177–1785. doi: 10.1016/j.ijrobp.2014.07.048.

Allison RR, Bagnato VS, Sibata CH (2010) Future of oncologic photodynamic therapy. Future Oncol 6(6):929–940

Azizian G, Riyahi-Alam N, Haghgoo S, Moghimi HR, Zohdiaghdam R, Rafiei B, Gorji E (2012) Synthesis route and three different core-shell impacts on magnetic characterization of gadolinium oxide-based nanoparticles as new contrast agents for molecular magnetic resonance imaging. Nanoscale Res Lett 7(1):549

Babaei M, Ganjalikhani M (2014) The potential effectiveness of nanoparticles as radio sensitizers for radiotherapy. Bioimpacts 4(1):15.

Bernard BK, Osheroff MR, Hofmann A, Mennear JH (1990) Toxicology and carcinogenesis studies of dietary titanium dioxide-coated mica in male and female Fischer 344 rats. J Toxicol Environ Health 29(4):417–429

Bischoff F, Bryson G (1982) Tissue reaction to and fate of par- enterally administered titanium dioxide. I. The intraperitoneal site in male Marsh-Buffalo mice. Res Commun Chem Pathol Pharmacol 38(2):279–290

Bump EA, Hoffman SJ, Foye WO, Abraham DJ (2003) Radiosensitizers and radioprotective agents. In: Abraham DJ (ed) Chemotherapeutic drugs, Burger's medicinal chemistry and drug discovery, Vol 5. John Wiley, New York, pp 151–211

Chatterjee DK, Fong LS, Zhang Y (2008) Nanoparticles in photodynamic therapy: an emerging paradigm. Adv Drug Deliv Rev 60(15):1627–1637

Fabian E, Landsiedel R, Ma-Hock L, Wiench K, Wohlleben W, van Ravenzwaay B (2008) Tissue distribution and toxicity of intravenously administered titanium dioxide nanoparticles in rats. Arch Toxicol 82(3):151–157

Fang C, Zhang M (2009) Multifunctional magnetic nanoparticles for medical imaging applications. J Mater Chem 19(35):6258–6266

Garnica-Garza HM (2009) Contrast-enhanced radiotherapy: feasibility and characteristics of the physical absorbed dose distribution for deep-seated tumors. Phys Med Biol 54(18) 5411–5425

Hainfeld JF, Slatkin DN, Focella TM, Smilowitz HM (2006) Gold nanoparticles: a new X-ray contrast agent. Br J Radiol 79(939):248–253

Huo S, Ma H, Huang K, Liu J, Wei T, Jin S, Zhang J, He S, Liang XJ (2013) Superior penetration and retention behavior of 50 nm gold nanoparticles in tumors. Cancer Res 73(1):319–330

Jin C, Tang Y, Yang FG, Li XL, Xu S, Fan XY, Huang YY, Yang YJ (2011) Cellular toxicity of TiO_2 nanoparticles in anatase and rutile crystal phase. Biol Trace Elem Res 141(1-3):3–15

Kim BY, Rutka JT, Chan WC (2010) Nanomedicine. N Engl J Med 363(25):2434–2443

Kim D, Yu MK, Lee TS, Park JJ, Jeong YY, Jon S (2011) Amphiphilic polymer-coated hybrid nanoparticles as CT/MRI dual contrast agents. Nanotechnology 22(15):155101

Leon S, Zdenka K, Kostya O, Shailesh K (2012) Nanoparticles in cancer imaging and therapy. J Nanomater Vol(2012), Article ID 891318

Maeda H, Wu J, Sawa T, Matsumura Y, Hori K (2000) Tumor vascular permeability and the EPR effect in macromolecular therapeutics: a review. J Control Release 65(1-2):271–284

Nakayama M, Sasaki R, Ogino C, Tanaka T, Morita K, Umetsu M, Ohara S, Tan Z, Nishimura Y, Akasaka H, Sato K, Numako C, Takami S, Kondo A (2016) Titanium peroxide nanoparticles enhanced cytotoxic effects of X-ray irradiation against pancreatic cancer model through reactive oxygen species generation in vitro and in vivo. Radiat Oncol 11(1):91

Perrault SD, Walkey C, Jennings T, Fischer HC, Chan WC (2009) Mediating tumor targeting efficiency of nanoparticles through design. Nano Lett 9(5):1909–1915

Service RF (2005) Materials and biology: Nanotechnology takes aim at cancer. Science 310(5751):1132–1134.

Srivastava SK, Yamada R, Ogino C, Kondo A (2013) Biogenic synthesis and characterization of gold nanoparticles by Escherichia coli K12 and its heterogeneous catalysis in degradation of 4-nitrophenol. Nanoscale Res Lett 8(1):70

Townley HE, Kim J, Dobson PJ (2012) In vivo demonstration of enhanced radiotherapy using rare earth doped titania nanoparticles. Nanoscale 4(16):5043–5050

Ruba T, Tamilselvi R (2018) Radiosensitizers and radioprotectors for effective radiation therapy–A review. Asian J Appl Sci Eng 2(1):77–86

Wilson BC, Patterson MS (2008) The physics, biophysics, and technology of photodynamic therapy. Phy Med Biol 53(9):R61–R109

Yamaguchi S, Kobayashi H, Narita T, Kanehira K, Sonezaki S, Kubota Y, Terasaka S, Iwasaki Y (2010) Novel photodynamic therapy using water-dispersed TiO_2 polyethylene glycol compound: evaluation of antitumor effect on glioma cells and spheroids in vitro. Photochem Photobiol 86(4):964–971

Yezhelyev MV, Gao X, Xing Y, Al-Hajj A, Nie S, O'Regan RM (2006) Emerging use of nanoparticles in diagnosis and treatment of breast cancer. Lancet Oncol 7(8):657–667

Yin JJ, Liu J, Ehrenshaft M, Roberts JE, Fu PP, Mason RP, Zhao B (2012) Phototoxicity of nano titanium dioxides in HaCaT keratinocytes—generation of reactive oxygen species and cell damage. Toxicol Appl Pharmacol 263(1):81–88

Figure Legends

Fig. 1 Characteristics of titanium dioxide nanoparticles (TiO_2-NPs) (a) Representative transmission electron microscopy image of the TiO_2-NPs. Their diameter is approximately 50 nm. (b) Size distribution of the TiO_2-NPs as measured using dynamic light scattering.

Fig. 2 Magnetization hysteresis loop of the titanium dioxide nanoparticles (TiO_2-NPs)

Fig. 3 Colony forming assay results after exposure of MIAPaCa-2 to graded dose of X-ray radiation combined with TiO_2-NPs. *P<0.05 and **P<0.1.

Fig. 4 (a, b) Computed tomographic images and the corresponding Hounsfield unit values of the titanium dioxide nanoparticles (TiO_2-NPs) (c, d) T_1-weighted magnetic resonance images and the corresponding T_1 relaxation rates ($1/T_1$) (e, f) T_2-weighted magnetic resonance images and the corresponding T_2 relaxation rates ($1/T_2$)

a)

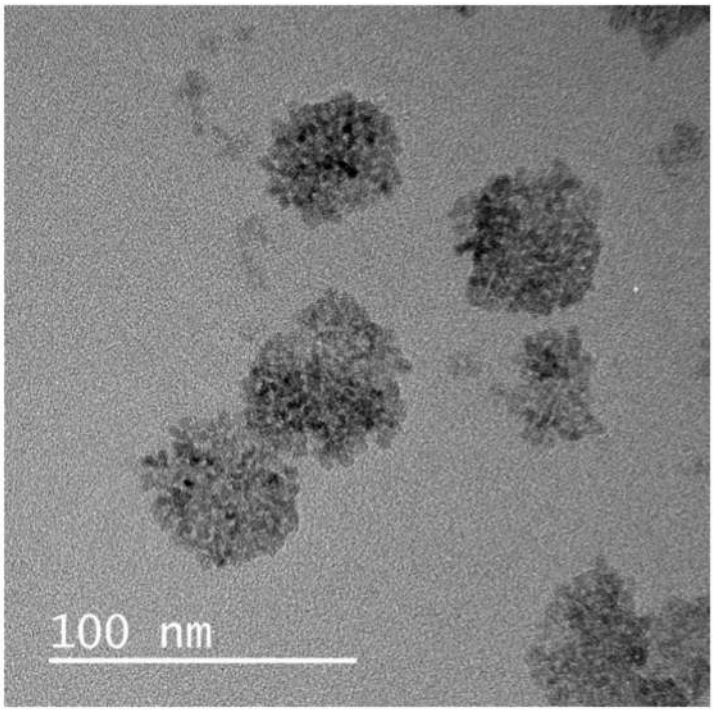

b)

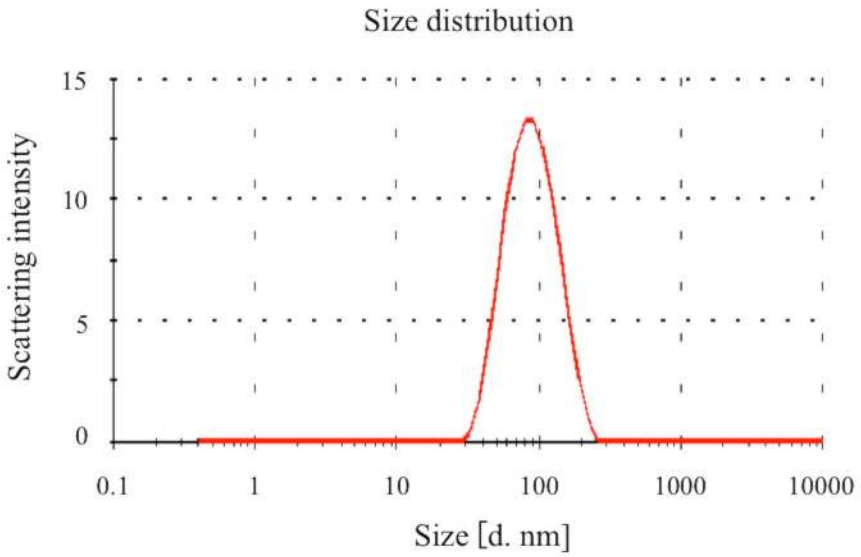

Fig.1 Akasaka et al.

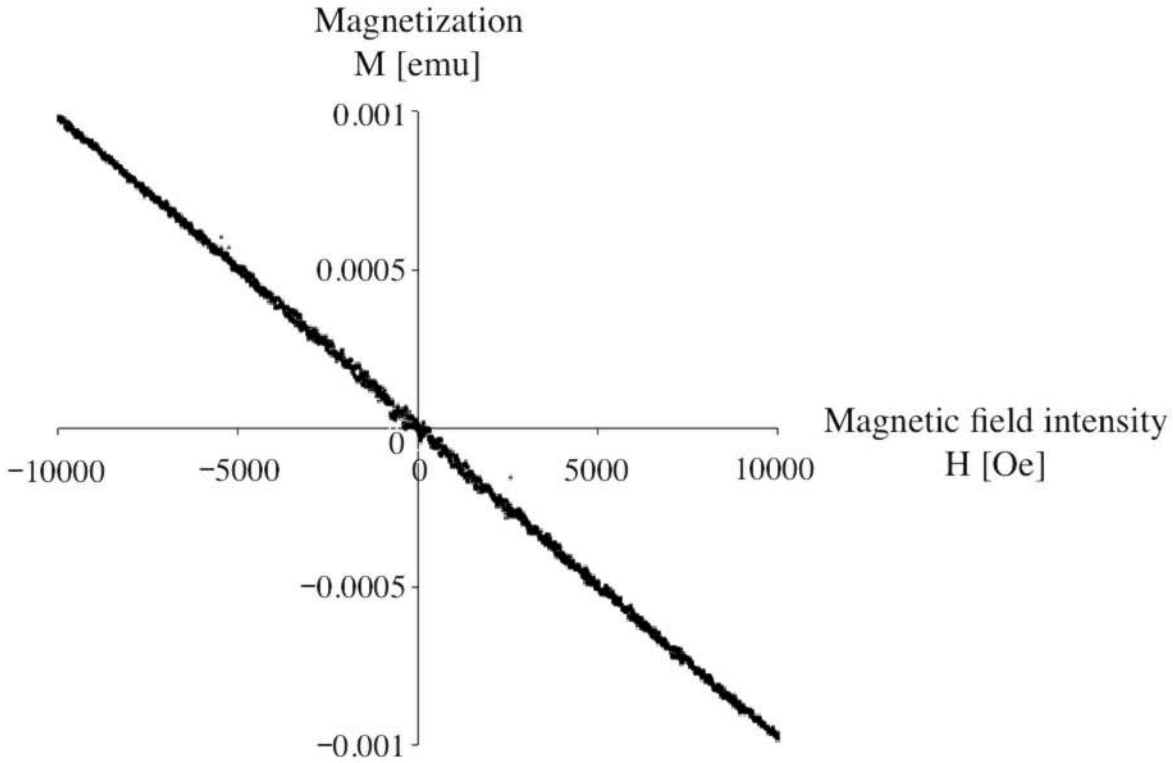

Fig.2 Akasaka et al.

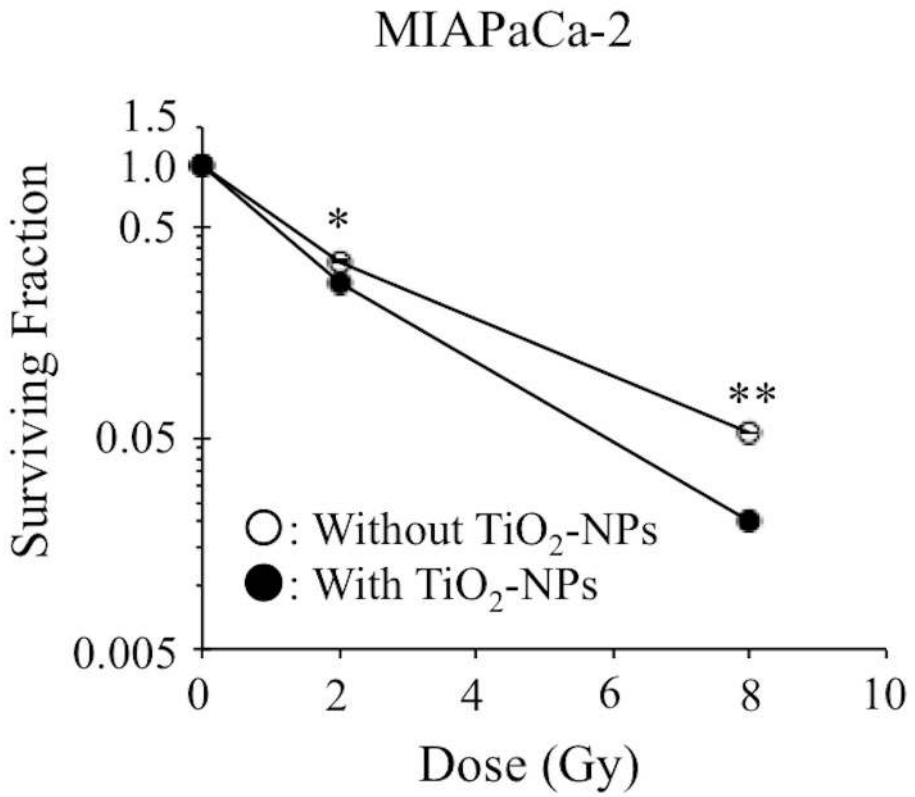

Fig.3 Akasaka et al.

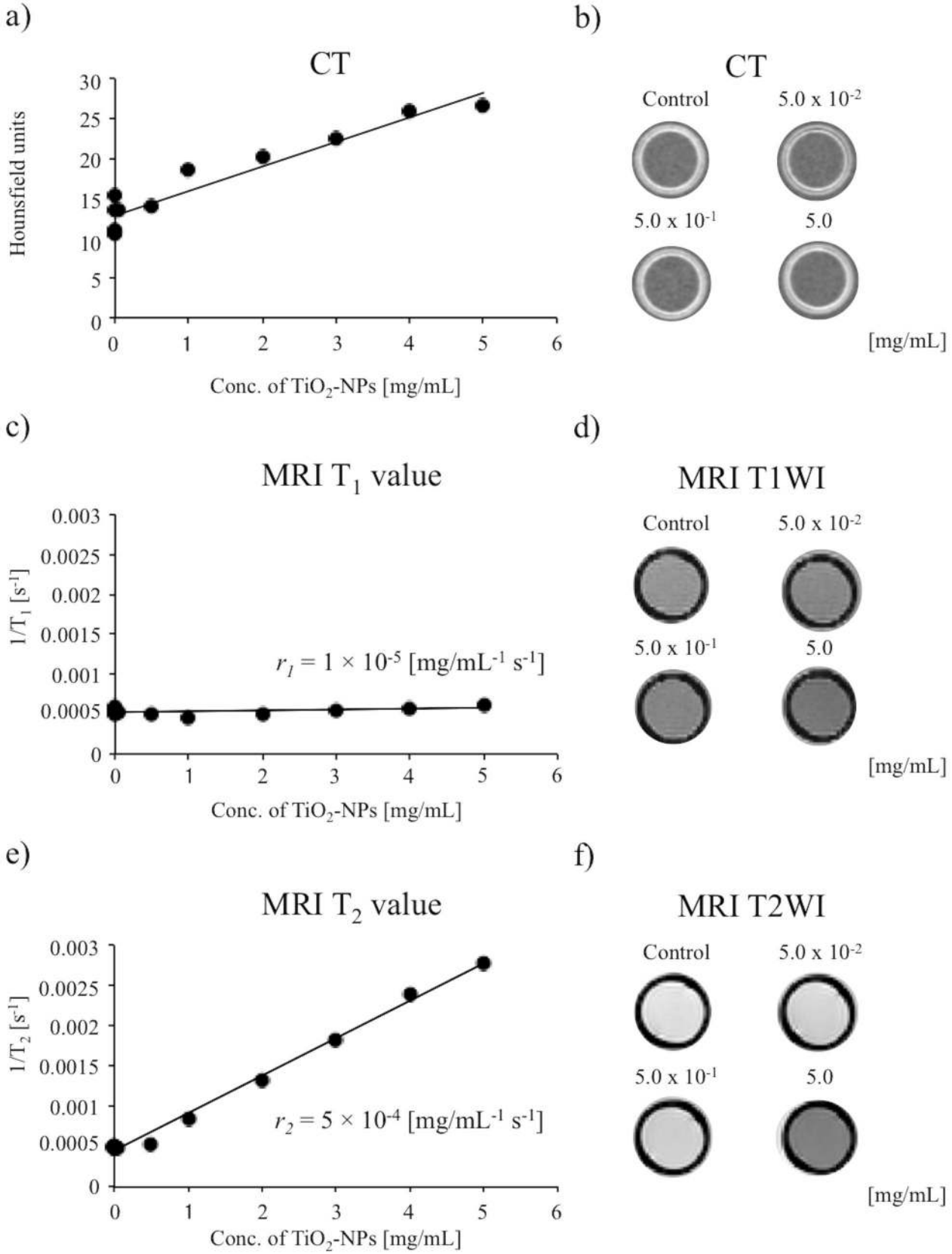

Fig.4 Akasaka et al.

Table 1. The CT values, T_1 values, and T_2 values of TiO_2-NPs at each concentrations.

Concentration of TiO_2-NPs [mg/mL]	CT value [HU]	T_1 value [msec]	T_2 value [msec]
0.0	13.4	1970.1	2046.8
5.0×10^{-6}	10.5	1811.5	2014.8
5.0×10^{-5}	10.8	1728.2	1974.8
5.0×10^{-4}	11.0	1715.6	1999.4
5.0×10^{-3}	15.3	1939.9	2046.8
5.0×10^{-2}	13.4	1905.3	2047.0
5.0×10^{-1}	13.9	2020.9	1895.4
1.0	18.5	2202.5	1191.2
2.0	20.1	1968.2	754.3
3.0	22.4	1810.9	548.1
4.0	25.8	1770.0	417.1
5.0	26.5	1614.4	360.8